# Response of Automated Tow Placed Laminates to Stress Concentrations

*Douglas S. Cairns[1], Larry B. Ilcewicz[2], and Tom Walker[2]*



***Abstract***

*In this study, the response of laminates with stress concentrations is explored. Automated Tow Placed (ATP, also known as Fiber Placement) laminates are compared to conventional tape layup manufacturing. Previous tensile fracture tests on fiber placed laminates show an improvement in tensile fracture of large notches over 20% compared to tape layup laminates. A hierarchial modeling scheme is presented. In this scheme, a global model is developed for laminates with notches. A local model is developed to study the influence of inhomogeneities at the notch tip, which are a consequence of the fiber placement manufacturing technique. In addition, a stacked membrane model was developed to study delaminations and splitting on a ply-by-ply basis. The results indicate that some benefit with respect to tensile fracture (up to 11%) can be gained from inhomogeneity alone, but that the most improvement may be obtained with splitting and delaminations which are more severe in the case of fiber placement compared to tape layup. Improvements up to 36% were found from the model for fiber placed laminates with damage at the notch tip compared to conventional tape layup.*

## Introduction

As advanced composites continue to be utilized in large, primary structures, a need exists to identify and quantify those parameters affecting fracture performance. Structures are typically manufactured from thin (0.127 mm) prepreg tape (305 mm wide), laminated and cured in an autoclave. Obviously, manufacturing large structures with even moderate volume production schedules will require alternative processing. One such alternative is Automated Tow Placement (ATP), also known as Fiber Placement (FP). This manufacturing technique has the advantage that fabrication production rates may be increased and the production may be automated. This fabrication method, as developed by Hercules, is shown in Figure 1.

In Figure 1, individual tows are placed on a creel and passed through a robotic head. A rotational axis, along with manipulation of the robotic head, allows placement of these individual tows. Unlike conventional filament winding, where compaction is provided via tensioning of the tows, fiber placement provides compaction via roller pressure. This versatility allows for manufacturing structures which are not axisymmetric and may even contain concave surfaces. Consequently, the designer is not constrained to near geodesic paths. In addition, individual tow cut and add allows for in-situ thickness control. These individual tows allow for intra-ply hybridization as well.

[1]Hercules Materials Company, Composite Products Group, Magna, UT
[2]Boeing Commercial Airplanes, Structures: Advanced Composites, Seattle, WA

This manufacturing process results in a tow to tow architecture which is different from standard prepreg tape laminated structures. Small gaps and laps can form between the tows, which are approximately 2.54 mm wide and between bands, which are 30 mm or greater. This can result in localized inhomogeneities. This is illustrated in Figure 2 for a $[-45/+45/90/+30/-30/\bar{0}]_s$ laminate configuration. Figure 2 is a Computer Aided Design (CAD) generated model of the ply by ply and tow by tow buildup in a localized region of a structure. Each line represents the boundary between tows. The regions where lines cross represent potential lap/gap sites. The minimum spacing is approximately 1.5 tow widths or 3.8 mm. As a result, this manufacturing process introduces another level of inhomogeneity which is greater than the thickness of individual plies. As with other alternative forms such as woven materials, it is improper to view fiber placement as a material form, especially with respect to fracture. Therefore, a need exists to understand the influence of this inhomogeneity on performance.

## Impetus

The fiber placement architecture can result in improved fracture properties under tensile loading applications as shown in Figure 3a [1,2]. This improvement in fracture is an important parameter for improving Boeing's advanced fuselage performance as shown in Figure 3b. This improvement has the largest influence on decreasing weight with improved costs compared to conventional prepreg tape laminates. The motivation behind this study is to understand the tensile fracture performance of fiber placed structures.

## Model Description

### Global Model

To study the influence of notches, a global two-dimensional finite element model was constructed. A mesh for this model is shown in Figure 4. The model is a half symmetry model (important later) about the left hand side, which is fixed vertically at the bottom and has a uniform vertical displacement at the top to simulate testing. This layup is AS4/3501-6 in a $[-45/+45/90/+30/-30/\bar{0}]_s$ stacking configuration [3]. The region of interest is near the tip of the crack. Hence, logarithmic mesh refinement was utilized at the tip.

For greater accuracy near the crack tip, a hybrid membrane element based on the Hellinger-Reissner principle $\Pi_R$ was used [4,5]. In this formulation, assumed fields for the stress and displacements are utilized.

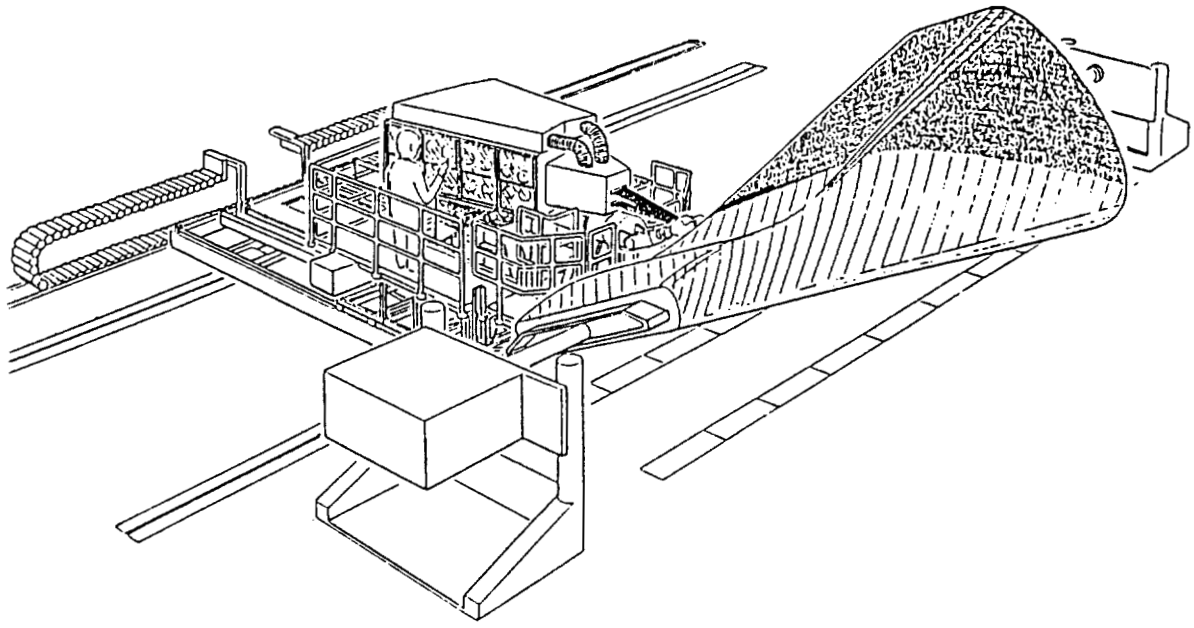

Figure 1. Fiber Placement (Automated Tow Placement) Process

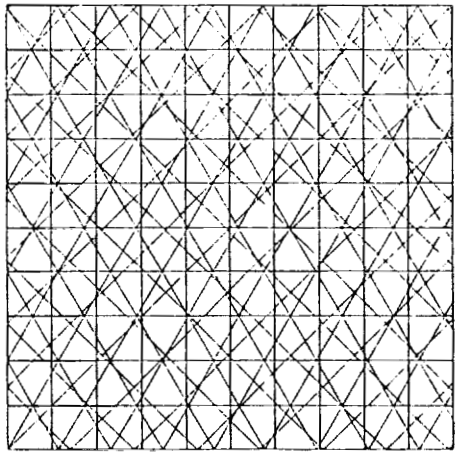

CAD-generated local region

25.4 mm X 25.4 mm Region, 2.54 mm tow width
[-45/+45/90/+30/-30/$\bar{0}$]s AS4/3501-6

Cross-over points represent potential lap (overlap) or gap (space) regions

Figure 2. Resulting Fiber Placement Architecture for [-45/+45/90/+30/-30/$\bar{0}$]$_s$ Laminate

Tension Residual Strength Curves Normalized By Material Density

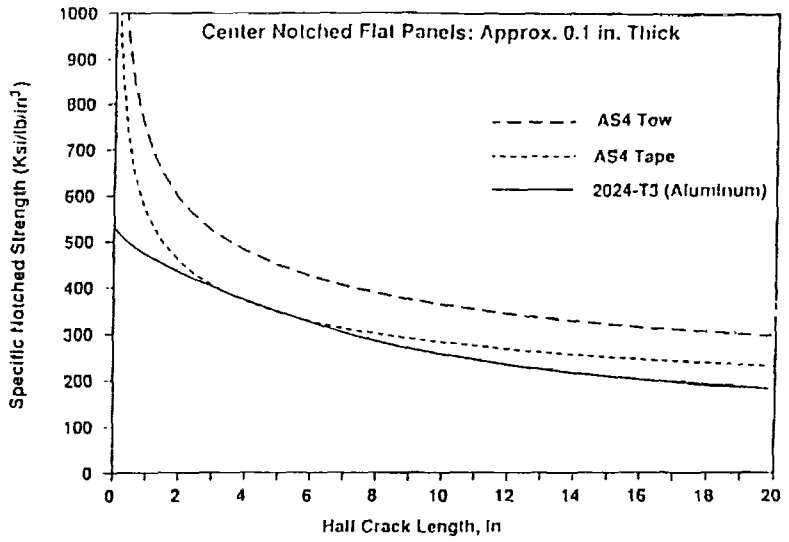


a) Improvement in Tensile Fracture

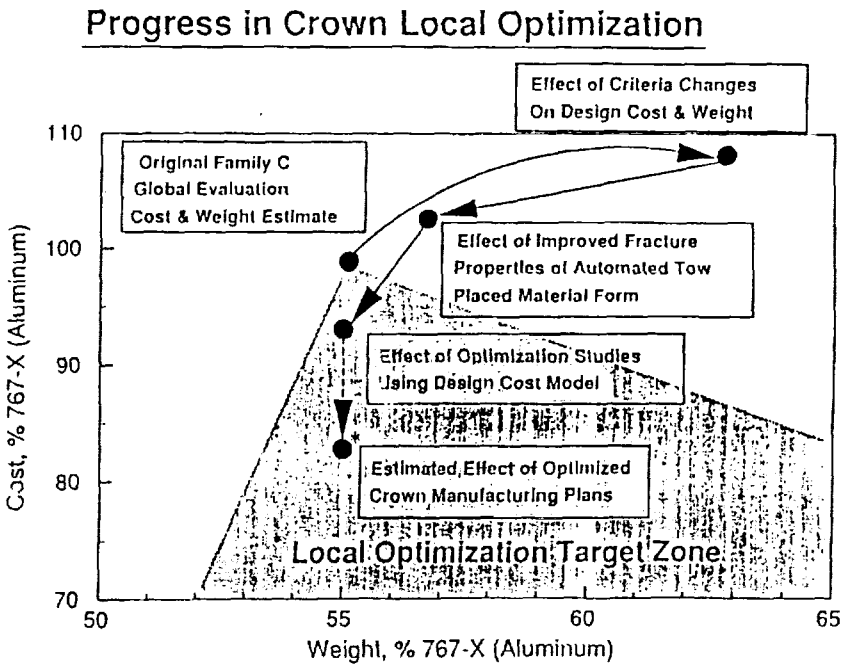


b) Impact of Improvement on Weight and Cost of Advanced Fuselage Structure

Figure 3. Improvement in Performance for Automated Tow Placement versus Tape

$$\sigma = P\beta \qquad a)$$
$$u = Nq \qquad b)$$
$$Du = Bq \qquad c)$$

$$\Pi_R = \int_V \left[ -\frac{1}{2}\sigma^T S\sigma + \sigma^T (Du) \right] dV \qquad d) \qquad (1)$$

where $\sigma$ is stress
P is the interpolating function for the stress
u is the displacement vector
N is the displacement interpolating function
q is the nodal displacement
D is the kinematic operator matrix
B is the operator matrix in terms of nodal displacements
S is the element compliance
and V is the elemental volume.

Invoking the stationary condition $\delta\Pi^R$ equal to zero and condensing out the $\beta$ parameters yields an elemental stiffness matrix **k**, in terms of the nodal displacements of the form:

$$k = G^T H^{-1} G \qquad a)$$

*where*

$$G = \int_V P^T B dV \qquad b) \qquad (2)$$

$$H = \int_V P^T S P dV \qquad c)$$

**Local Model**

The local model is illustrated in Figure 5. This model is a half symmetry, 25.4 mm high by 50.8 mm wide. The darkened areas represent elements which have different membrane stiffness properties to represent laps or gaps. To bound the problem with respect to inhomogeneity, laps were modeled as double stiffness regions, while the gaps were modeled as resin regions. The distance between laps/gaps represents the minimum inhomogeneity spacing. The elements are sized to approximate the 0.76 mm maximum lap/gap which is specified in fiber placement.

Displacements were invoked around the perimeter from least squares fitting of the displacements obtained from the global model. The local model is slightly more compliant than the global model. Consequently, an error norm ratio for stresses along the perimeter in the global region and the local region was constructed. The results were multiplied by this first order correction [6].

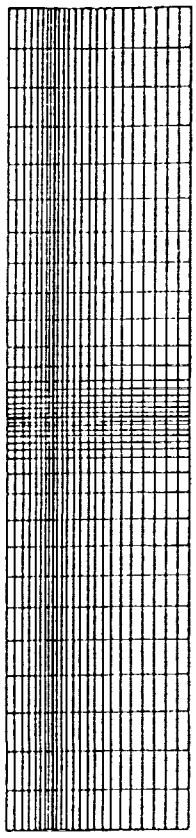


Global Model Description

559 mm long, 254 mm wide,
63.5 mm central notch,

Symmetry about Y-axis
Uniform Y displacement at top,
Fixed in Y at bottom

4 node isoparametric
displacement, 5 beta assumed
stress hybrid elements

Figure 4. Global Finite Element Mesh

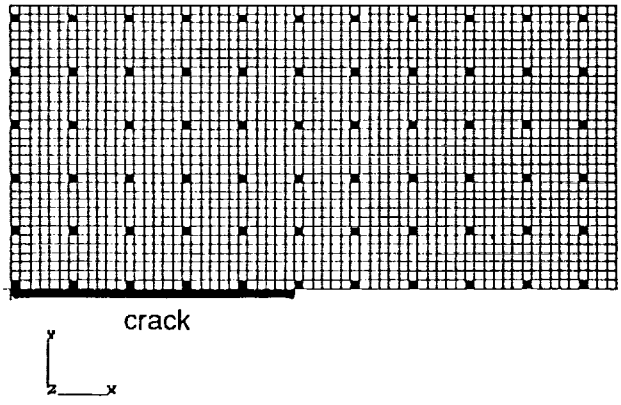


Local Model Description

50.8 mm X 25.4 mm local model
symmetry about X axis
perimeter displacements from
Global model

darkened areas represent
local lap/gap sites
gap - resin
lap - higher stiffness
inclusion

larger areas varied to simulate
hybrid panels

Figure 5. Local Finite Element Mesh
(darkened areas represent areas of inhomogeneity)

**Failure Criterion - Basis for Comparisons**

The Whitney-Nuismer Average Stress Criterion was implemented on a strain basis to compare the results between models in the near field region [7]. This was implemented as:

$$SR = \frac{\epsilon_0}{\frac{1}{a_0}\int_{a}^{a+a_0} \epsilon(r,\theta)\,dr} \tag{3}$$

where SR is the ratio of far-field strain to near-field strain
$\epsilon_0$ is the far-field strain of interest
$a_0$ is the averaging parameter (assumed to be a material constant)
and $\epsilon(r,\theta)$ is the strain along a path in the critical direction
(not necessarily perpendicular to the applied load)

Using a progressive failure criterion, the failure of the $0^0$ ply in the $[-45/+45/90/+30/-30/0]_s$ laminate was determined to be critical. This fiber-dominated failure was utilized as the basis of comparison.

## Results

**Influence of Inhomogeneity**

As stated above, the fiber placement process results in an architecture which has local inhomogeneities. To determine the effect of these inhomogeneities, the local model was used to determine average strain near the crack tip. An averaging parameter $a_0$ of 3.81 mm was used based on previous tests on AS4/3501-6 [8]. The near-field $\epsilon_y$ strain isocontours are shown in Figure 6a. This strain field is a classical plane stress isocountour. In Figure 6b is the strain field for gaps (resin areas, i.e. compliant inclusions) in the darkened regions shown in Figure 5. Notice that small perturbations in the strain field can be seen around the perimeter of the isocountours. The case where all of the inhomogeneity sites are laps (double thickness membrane regions, i.e. stiff inclusions) is shown in Figure 6c. Large perturbations in the strain isocontours can be seen here.

The average strain in the case of laps divided by the baseline average strain is approximately 0.97. The average strain ratio for the case of laps (stiff inclusions) was found to be 0.89. Consequently, a slight improvement over the baseline results can be expected to be gained on the basis of inhomogeneity alone.

A model of intraply glass/carbon hybrids was also conducted. The fiber placement process allows for introducing intraply hybridization via individual tows. This results in large, inhomogeneous regions. Large all carbon regions exist, and no benefit for local average strain results was found for the case of intraply hybridization. The relative improvement for inhomogeneity is shown in Figure 7.

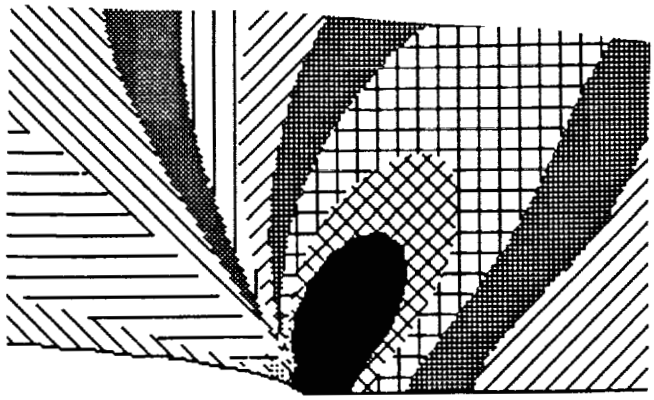

a) Baseline (homogeneous case, smooth strain isocontours)

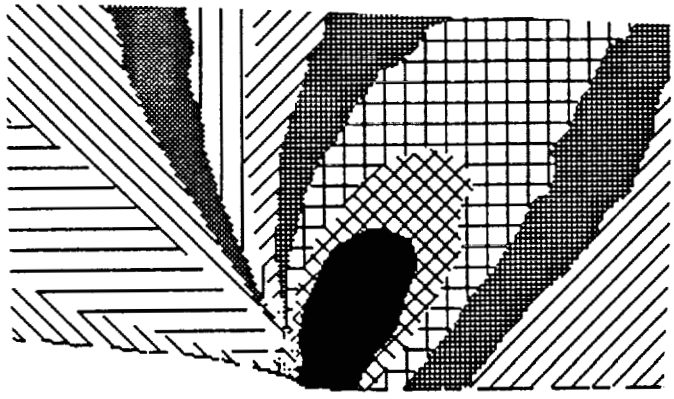


b) Gaps (resin pocket inhomogeneities from gap, small perturbation in strain)

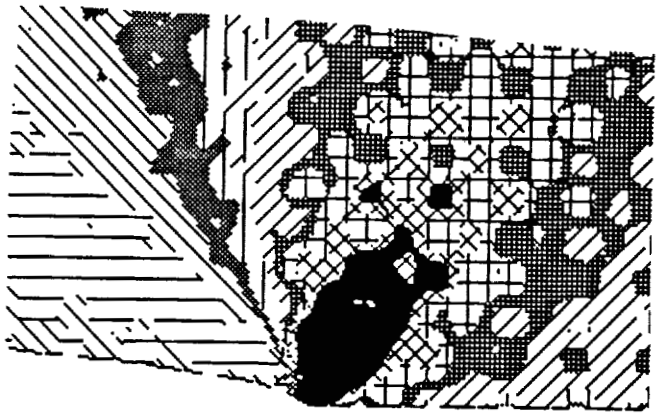

c) Laps (stiff inclusion from overlap, large perturbation in strain)

Figure 6. Local Inhomogeneity Effect on Strain Field

It is important to note that these studies are bounding cases. That is, the assumptions of proximity and buildup of laps/gaps is rather severe. Actual improvement from inhomogeneity alone can be expected to be less. The experimentally determined ratio of fiber placed laminates to tape laminates is approximately 0.795 as shown in Figure 3a. This is much better than the 0.89 ratio determined for the case of laps. Consequently, the influence of inhomogeneity on the strain field alone cannot completely explain the benefits. This does not, however, preclude the inhomogeneity from affecting the damage type and progression during fracture.

**Influence of Damage**

The results above indicate that inhomogeneity is not solely responsible for the improvement from tape to tow. Clearly, some other mechanisms provide the improvements. While the inhomogeneity has a moderate influence on the strain field, it is expected to have a large influence on damage progression during fracture. In Figure 8 are shown dye-enhanced radiographs of tape layup and fiber placed, notched, fractured laminates. Notice the much larger damage zone ahead of the crack tip in the case of fiber placed laminates compared to the tape layup laminates at final fracture. This damage size is on the order of the size of the original notch. The influence of laps/gaps on splitting and delamination has been postulated previously [1,2]. The goal here is to quantify the influence of these damage types on final fracture.

The damage produced is three dimensional. Different plies split and delaminate. A complete, three dimensional model of these damage types would be quite complicated. To model splitting and delaminations with some degree of pragmatism, a stacked membrane model was developed. In this model, membrane elements are stacked to simulate ply-by-ply lamination. Delaminations were introduced by releasing nodes through the thickness. Splitting was introduced by releasing nodes in the plane [9]. Therefore, while interlaminar stresses cannot be accurately modeled, the influence of constraints by surrounding plies and material can be modeled in the plane of a ply. This technique was found to be simple and practical. The stacked membrane region is illustrated in Figure 9. Here, the half-symmetry is necessary, since the presence of membrane extensional-shear coupling ($A_{16}$ and $A_{26}$ in classical laminated plate theory) may be important.

Splitting alleviates the influence of the sharp notch and acts as a crack blunting mechanism in composites. This is illustrated in Figure 10. The surrounding plies are shown in Figure 10a, while deformation of the $0^0$ ply is shown in Figure 10b. The node is released adjacent to the notch allowing shear lag to occur. Various splitting lengths were modeled (up to 0.8 times the notch length of 2a). Delaminations also alleviate the influence of the notch. The delamination allows plies to deform independently. This can also lower strains ahead of the notch. A variety of delamination sizes were modeled (up to 0.8 times the notch length of 2a).

Combined splitting plus delaminations provides the most benefit. In Figure 11 is illustrated the deformation of surrounding plies and the $0^0$ ply with a split plus delaminations in the surrounding plies. Notice that the material ahead of the crack tip

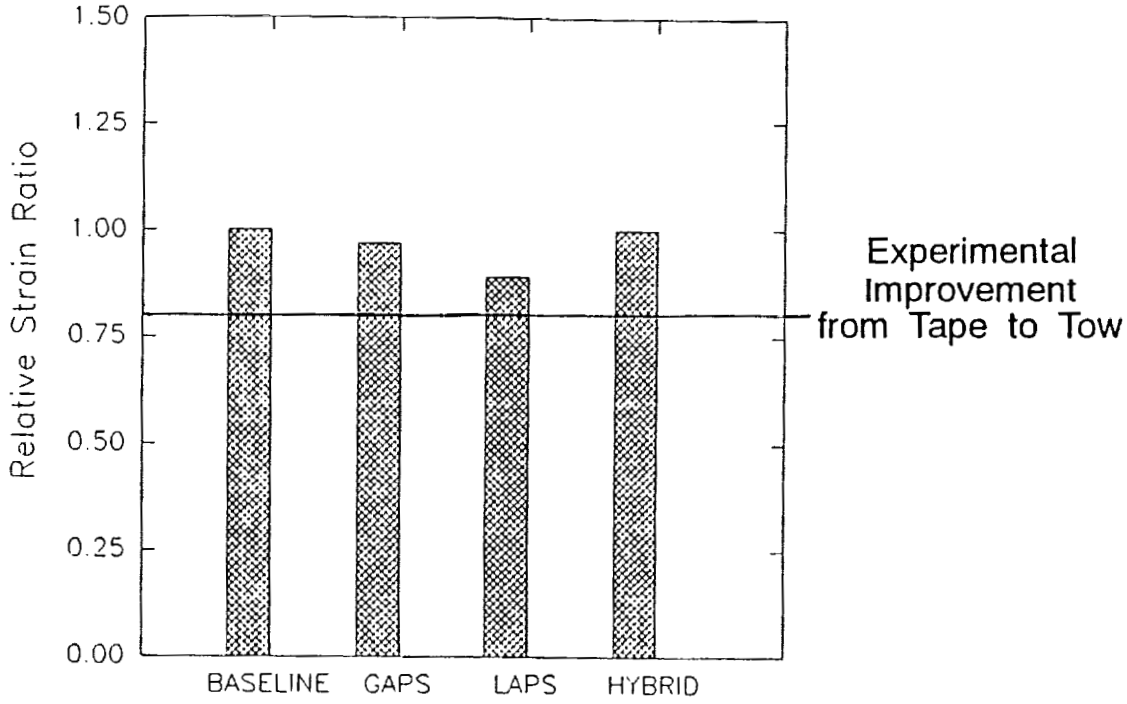


Figure 7. Local Inhomogeneity Effect on Tensile Fracture Performance

a) Tape Layup
(small damage zone)

b) Fiber Placed
(larger damage zone)

Figure 8. Dye-Enhanced Radiograph of Notch
Damage Differences Between Tape and Tow

*Original figure unavailable.

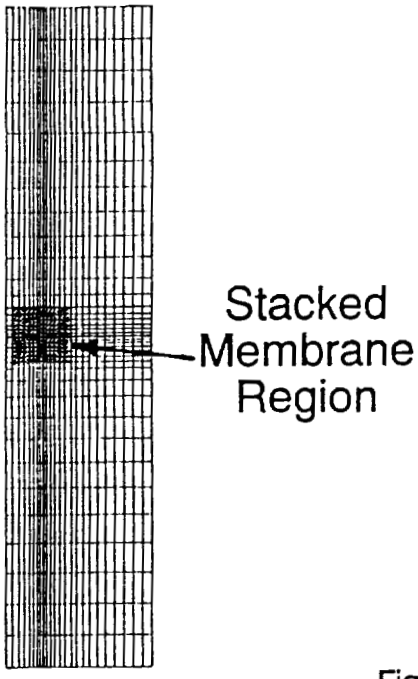


Model Features

Stacked membrane region for ply-by-ply analysis

Damage Modeling

Interply connectivity released to simulate delaminations

Intraply connectivity released to simulate splitting

Combinations

Relative average strain utilized for comparisons

Figure 9. Stacked Membrane Model

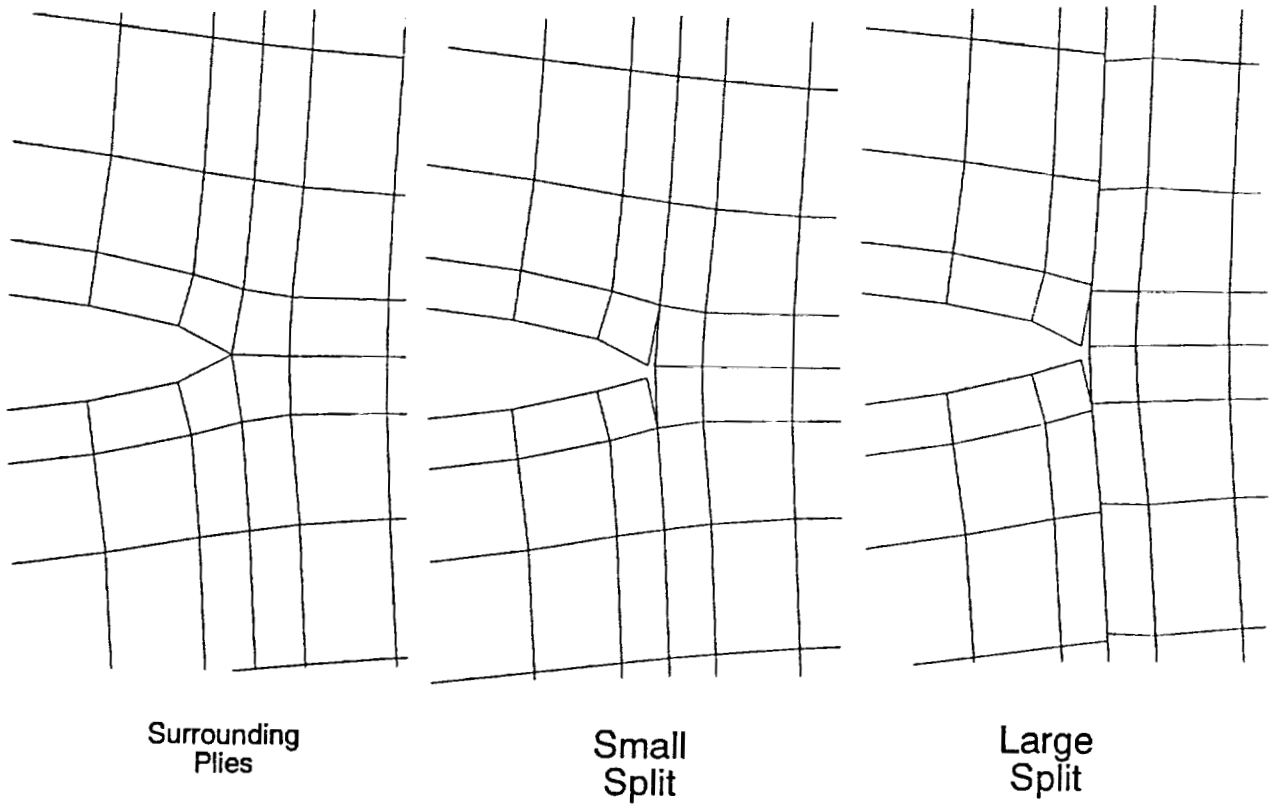


Figure 10. Splitting at Notch Tip

acts almost completely independently from the material behind the crack tip. This deformation is plotted on the same scale as shown for Figure 9.

Isocountours for the $\epsilon_y$ strain are shown in Figure 12. The surrounding plies again exhibit classical plane stress behavior in Figure 12a, while the split ply distributes strain over a larger region in Figure 12b. Also, the isocountours are much more uniform than in Figure 12a. Higher, localized strains can be seen above and below the crack as stress is reintroduced via shear lag.

The influences of these various damage types on average strain compared to baseline results are shown in Figure 13. The Sqrt [d/a] is the square root of the half damage size divided by original half crack length. For all damage types, the damage has little effect, until a large enough damage size is present to redistribute the local strain field. This occurs between Sqrt [d/a] equal to 0.2 to 0.4. Splits alone or delaminations alone cannot explain the benefit of experimentally observed improvement from tape to tow. A combination of damage types provides the most benefit.

## Conclusions and Recommendations

A study of the influence of inhomogeneity and damage on the tensile fracture performance of structures manufactured from fiber placement has been conducted. A global hybrid finite element model was constructed, and a local inhomogeneity model was constructed to explore strain fields near the crack. The results indicate that inhomogeneity can provide some benefit, but cannot completely explain the experimentally observed improvement in tensile fracture of laminates manufactured from conventional prepreg tape to laminates manufactured from fiber placement. A ply-by-ply stacked membrane model was utilized to study the influence of splitting, delaminations, and combined damage. The stacked membrane approach was found to be a practical two-dimensional method of analyzing damage which is essentially three dimensional. Additional configurations need to be examined to determine limitations. The influence of damage types, which are enhanced with fiber placement appears to play a greater role in the improvement compared to the inhomogeneity effects alone. Splitting provides some improvement, as well as delaminations. However, up to 36% improvement was provided by combined delaminations and splits for the damage sizes studied here. This interesting phenomenon warrants further research. In particular, while the enhancement from fiber placement is clearly beneficial for tensile fracture, it is necessary to determine if these damage types are beneficial for fracture of structures loaded in compression and shear as well.

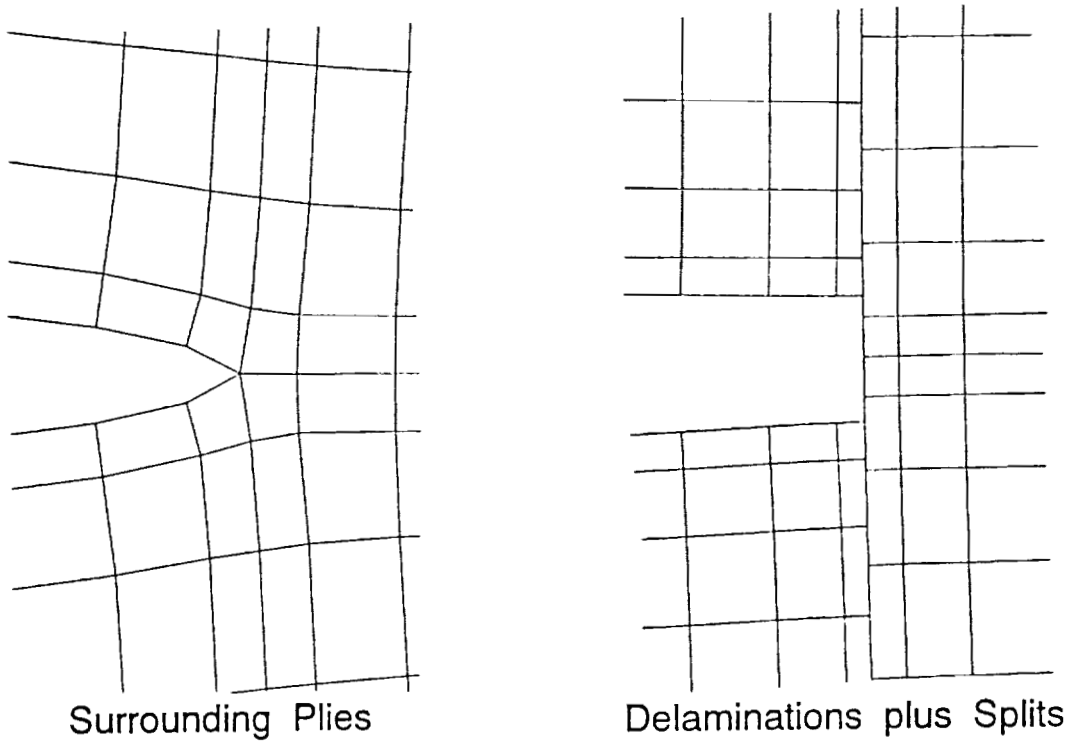


Figure 11. Delaminations plus Splits

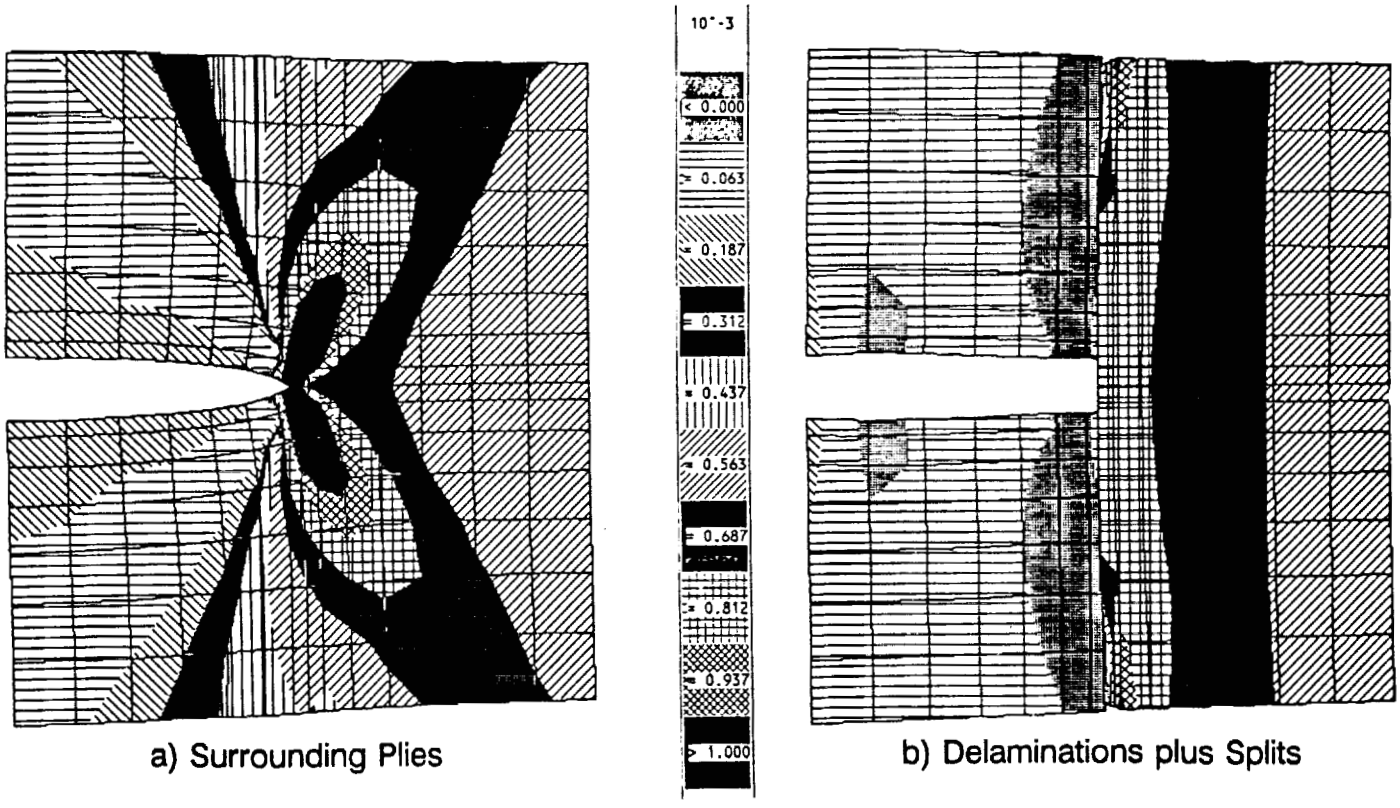


Figure 12. Isostrain Contours with Splitting Plus Delaminations

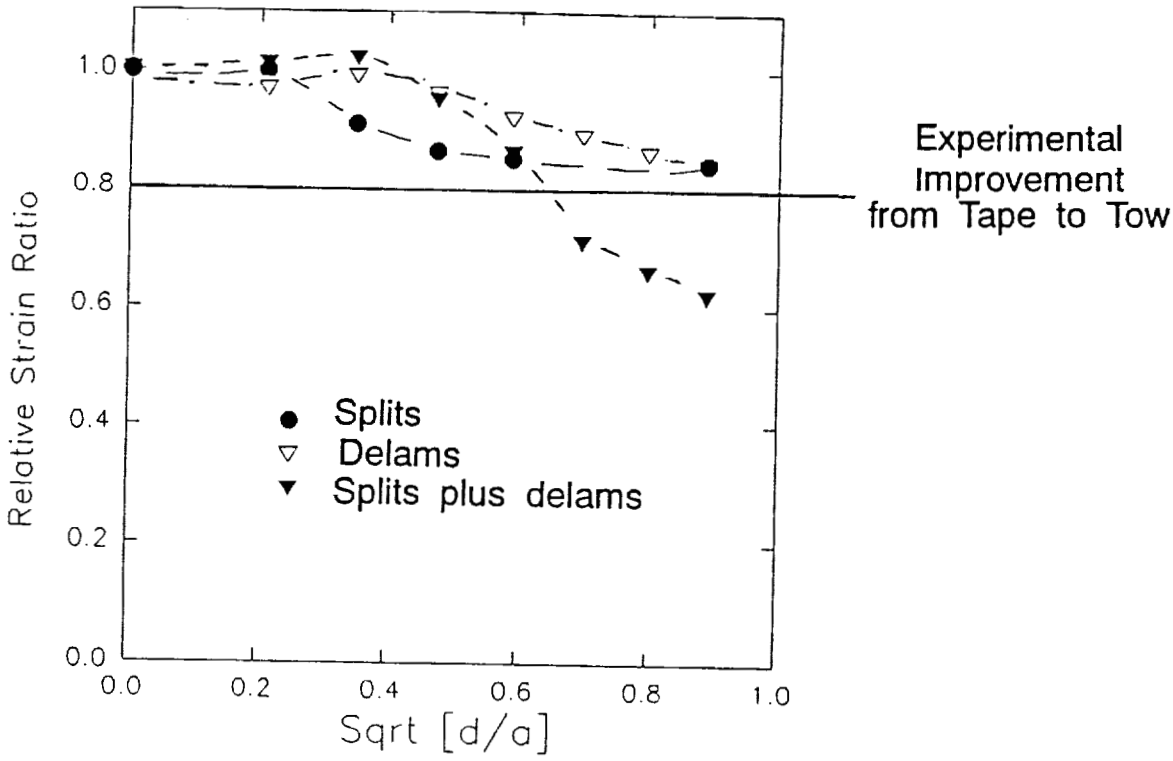


Figure 13. Improvement in Fracture for Various Damage Types

## References


1. Walker, T., Avery, W., Ilcewicz, L., Poe, C.C., Jr., and Harris, C.E., "Tension Fracture of Tow-Placed Laminates for Transport Applications", **Ninth DoD/NASA/FAA Conference on Fibrous Composites in Structural Design**, November 4-7, 1991.

2. Walker, T. and Ilcewicz, L.B., "Mechanical Tests and Analysis Predictions," **Proceedings of the Boeing/NASA review of ATCAS**, Contract NAS1-18889, May 15, 1991.

3. **Hercules Prepreg Tape Materials Characterization Data Package**, Fibers: AS4, IM6, IM7 & IM8, Resins: 8551-7, 8551-7A, 8552, 3501-6, Hercules Composite Products Group, Magna, Utah, November, 1988.

4. Washizu, K., **Variational Methods in Elasticity and Plasticity**, Third Edition, Pergammon Press, Elmsford, New York, 1982.

5. Pian, T.H.H., "Derivation of Element Stiffness Matrices by Assumed Stress Distributions," **AIAA Journal**, Vol. 5, No. 1, 1964, pp. 1333-1336.

6. Cook, R.D., **Concepts and Applications of Finite Element Analysis**, John Wiley and Sons, New York, New York, 1981, pp. 210-211.

7. Whitney, J.M. and Nuismer, R.J., "Stress Fracture Criteria for Laminates Containing Stress Concentrations," **Journal of Composite Materials**, Vol. 8, 1974, pp. 253-265.

8. Cairns, D.S. and Lagace, P.A., "Residual Tensile Strength of Graphite/Epoxy and Kevlar/Epoxy," **Composite Materials: Testing and Design (Ninth Conference)**, American Society for Testing and Materials, Reno, NV, 1988.

9. Kortschot, M.T. and Beaumont, P.W.R., "Damage-Based Notch Strength Modeling: A Summary," **Composite Materials: Fatigue and Fracture (Third Volume)**, ASTM STP 1110, T.K. O'Brien, Ed., American Society for Testing and Materials, Philadelphia, 1991, pp. 596-616.